Available online at www.sciencedirect.com
SCIENCE DIRECT
Chemical Physics Letters 422 (2006) 51–57
CHEMICAL PHYSICS LETTERS
www.elsevier.com/locate/cplett

High resolution O 1s photoelectron shake-up satellite spectrum of H_2O

R. Sankari [a,b], M. Ehara [c,1], H. Nakatsuji [c], A. De Fanis [d], H. Aksela [a], S.L. Sorensen [e], M.N. Piancastelli [f], E. Kukk [b,g], K. Ueda [g,*]

[a] Department of Physical Sciences, P.O. Box 3000, 90014 University of Oulu, Finland
[b] Department of Physics, Materials Science, University of Turku, Finland
[c] Department of Synthetic Chemistry and Biological Chemistry, Graduate School of Engineering, Kyoto University, Nishikyo-ku, Katsura, Kyoto 615-8510, Japan
[d] SPring-8/JASRI, Sayou-gun, Hyogo 679-5198, Japan
[e] Department of Synchrotron Radiation Research, Institute of Physics, University of Lund, Box 118, S-221 00 Lund, Sweden
[f] Department of Physics, Uppsala University, Box 530, S-751 21 Uppsala, Sweden
[g] Institute of Multidisciplinary Research for Advanced Materials, Tohoku University, Sendai 980-8577, Japan

Received 12 January 2006; in final form 6 February 2006
Available online 28 February 2006

Abstract

The O 1s photoelectron satellite spectrum of water has been recorded with high resolution and some vibrational structures were detected. The electronic and vibrational structures observed in the experimental spectrum are well interpreted with the aid of the molecular ab initio calculations based on the symmetry adapted cluster-configuration interaction (SAC-CI) method.

1. Introduction

The interest in photoelectron shake-up satellite spectra of various atoms and molecules increased strongly at early 1970s [1,2], soon after the first gas phase ESCA studies of Siegbahn and coworkers [3]. The appearance of the shake-up states in the experimental photoelectron spectra was successfully explained by the electron correlation effects [4]. Despite the apparent simplicity of the phenomenum, it took a long time to achieve quantitative agreement between the experimental and theoretical data even on atoms [5]. Presently theoretical study of the molecular inner-shell shake-up spectra in quantitative accuracy is still a challenging subject [6–8].

In the case of water (H_2O), the structures of the experimental O 1s shake-up spectrum, recorded by Siegbahn [1], were theoretically studied first by Svensson et al. [9]. The calculations based on limited configuration interaction (CI) approach provided theoretical binding energies of the shake-up states and intensities of the relevant transitions. Also the main features of the spectrum could be assigned to single excitations related to the O 1s ionization. The subject was revisited later in the studies of Wahlgren [10], Creber et al. [11], Arneberg et al. [12] and Ågren and Carravetta [13]. In all these studies, the assignments of the states agreed mostly with one another. These theoretical works also reproduced reasonably the experimental spectra [1,14]. However, precise interpretation of the detailed structure is still difficult: the effect of electron correlations is inherently important in the theoretical description of the inner-shell shake-up satellite spectrum. The resolution of the latest published O 1s shake-up spectrum presented by Nordfors et al. [15] was still limited by the use of monochromatized X-ray source and this lack of high resolution experimental spectrum has hindered a more critical comparison between experimental and theoretical photoelectron satellite spectrum of H_2O. The comparison of earlier H_2O and D_2O spectra [15] seems to indicate that vibrational components exist in the satellite spectrum: the two spectra differ slightly in the widths of the structures. According to earlier experiments it

* Corresponding author. Fax: +81 22 217 5405.
E-mail address: ueda@tagen.tohoku.ac.jp (K. Ueda).
[1] Fax: +81 75 383 2741.

0009-2614/$ - see front matter © 2006 Elsevier B.V. All rights reserved.
doi:10.1016/j.cplett.2006.02.018

was also clear that the states obtained theoretically can be vibrationally broadened but none of the studies concentrated in detail on that issue.

In the present work, the O 1s photoelectron satellite spectrum of H_2O is recorded with unprecedented experimental resolution, employing monochromatized synchrotron radiation as a light source: the obtained high-resolution spectrum exhibits vibrational structure. The experimental spectrum is then compared with the ab initio spectrum, which is also obtained in the present work, employing the symmetry adapted cluster-configuration interaction (SAC-CI) general-*R* method [16–19]. In the series of applications, the SAC-CI general-*R* method was found to reproduce the fine details of the valence [20,21] and inner-shell ionization spectra [7,22]. Thus it is of interest to find out also how the SAC-CI method can be compared with other theoretical methods [9–13] applied to earlier investigations of the O 1s photoelectron satellite spectrum in H_2O. Furthermore, extensive calculations are performed for the potential energy curves and the vibrational structure of the shake-up states is examined. Recently, the same method was applied successfully to interpret the vibrational structure in the O 1s photoelectron mainline of H_2O [23]. The present task is, however, more challenging, since the earlier calculations (e.g. Ref. [12]) predicted that the shake-up states are strongly mixed. Thus, the present task is a more stringent test for the SAC-CI general-*R* method. We find that the method is capable of simulating the O 1s photoelectron satellite spectrum of H_2O and elucidating the vibrational structure.

2. Experimental

The measurements were carried out at the c branch of the beamline 27SU at SPring-8, a synchrotron radiation facility with an 8-GeV storage ring in Japan. The figure-8 undulator installed in this beamline produces high-intensity linearly polarized soft X-rays. When integer order (i.e. 1st, 2nd, ...) harmonics of the undulator radiation are chosen, the light is horizontally polarized whereas the half-integer (i.e. 0.5th, 1.5th, ...) harmonics provide vertically polarized light [24]. The radiation is guided to a Hettrick type monochromator that covers the photon energy range of 150–2500 eV with three different gratings. A more detailed description of the beamline and the monochromator can be found elsewhere [25,26]. The photon energy scale was calibrated using the CO_2 excitation energies reported by Prince et al. [27].

The ejected electrons were analyzed with an SES-2002 electron energy analyzer equipped with a gas cell: both were manufactured by Gammadata-Scienta Ab. The binding energy scale was calibrated by measuring the O 1s spectrum of O_2, whose binding energy values were measured by Sorensen et al. [28] with an accuracy of ± 0.02 eV. The analyzer broadening corresponding to 300 μm entrance slit and 100 eV pass energy is about 95 meV (FWHM). The photoelectron satellite spectrum was recorded at 650 eV photon energy with the photon bandwidth of approximately 95 meV. The overall experimental broadening, including Doppler broadening [29], was thus estimated to be about 135 meV, except in the high-resolution scan where the experimental broadening was about 110 meV. The transmission of the electron spectrometer was checked at the kinetic energy region of interest and it was found to be constant within a few percent.

3. Calculations

The ground state H_2O molecule belongs to C_{2v} point group ($R_{O-H} = 0.958$ Å; $\theta_{H-O-H} = 104.4°$) and its electronic configuration is

$$1a_1^2\ 2a_1^2\ 1b_2^2\ 3a_1^2\ 1b_1^2\ (^1A_1),$$

where $1a_1$ and $2a_1$ are almost pure O 1s and 2s orbitals, respectively, while $1b_2$ and $3a_1$ represent bonding orbitals and $1b_1$ is the out-of-plane non-bonding orbital.

In the process of simulating theoretical photoelectron satellite spectrum, the flexible basis set was used to describe the orbital reorganization and the electron correlations of

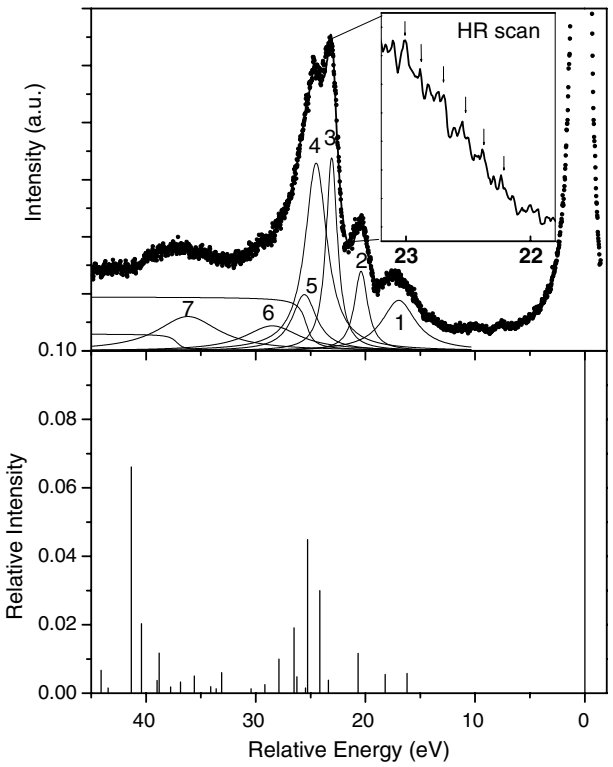

Fig. 1. *Upper panel:* Experimental O 1s photoelectron satellite spectrum of H_2O excited at 650 eV photon energy. Dots show the experimental data taken at 0° relative to polarization vector of incident radiation. Dotted lines represent the individual fitted components. The inset presents the high-resolution spectrum of the region labeled a. Thin vertical arrows drawn by eye indicate the observed vibrational components. *Lower panel:* Theoretical O 1s photoelectron satellite spectrum of H_2O. The columns show the energies and the intensities of the electronic transitions. In both panels, the energy is given relative to the binding energy of the O 1s mainline.

the inner-shell ionized state; TZV [5s3p/3s] of Ahlrichs' group [30] augmented with polarization d-function ($\zeta_d = 0.85$) for O. Rydberg functions [2s2p] for $n = 3$ and [1s1p] for $n = 4$ of Dunning [31] were also added. The following notation for the molecular orbitals (MOs) was chosen: occupied core MO ($1a_1$), occupied valence MOs ($2a_1$, $1b_2$, $3a_1$ and $1b_1$), $n = 3$ Rydberg orbitals ($6a_1$, $7a_1$, $3b_1$ and $3b_2$), $n = 4$ Rydberg orbitals ($4a_1$, $5a_1$, $2b_1$ and $2b_2$), anti-bonding MOs ($8a_1$, $4b_2$), the rest of the MOs were virtual orbitals due to TZV basis and polarization function. In some cases, higher virtual MOs like $4b_1$ also describe the $n = 3$ Rydberg with the linear combination.

The inner-shell satellite spectrum was calculated by the SAC-CI general-*R* method [19]. Since the shake-up states are dominantly described by double and triple excitations, the *R*-operators were included up to quadruples. All the MOs were included in the active space for describing the core–hole relaxation. In order to reduce the computational effort, perturbation selection procedure was adopted [32]. Reference functions for selections were chosen from the small-active-space SDT-CI vectors to guarantee the accuracy for the satellite spectra. The threshold of the linked terms for the ground state was set to $\lambda_e = 1.0 \times 10^{-7}$ and the unlinked terms are adopted as the products of the important linked terms whose SD-CI coefficients were larger than 0.005. For the ionized state, all the single and double operators are included and the energy threshold of triples and quadruples was set to $\lambda_e = 1.0 \times 10^{-8}$. The thresholds of the CI coefficients for calculating the unlinked operators in the SAC-CI method were 0.05 and 0.0 for the *R* and *S* operators, respectively.

For analyzing the fine structure of the spectra, two dimensional (2D) potential energy surfaces were calculated for the low-lying 15 A_1 states; one main line and 14 shake-up satellite states were examined. The symmetric stretching and bending motions were examined for the geometries of $R_{O-H} = 0.9$–1.45 Å and H–O–H angle $\theta_{H-O-H} = 100$–$180°$ at the C_{2v} structure. Non-symmetric C_s structure was also examined; $R_{O-H_1} = 1.10$–1.50 Å with $R_{O-H_2} = 1.15$ Å and $\theta_{H-O-H} = 130°$. For these calculations, the DZ plus Rydberg functions [2s2p] for $n = 3$ were used and the perturbation selection was not performed in the SAC-CI calculations with *R*-operators included up to quadruple operators.

The SAC/SAC-CI calculations were executed with the GAUSSIAN03 suite of programs [33] with some modifications for calculating the inner-shell ionization spectra. Theoretical ionization cross-sections were calculated using the monopole approximation to estimate the relative intensities of the peaks. Both initial-state and final-ionic-state correlation effects were included.

Table 1
Experimental energies and intensities of the O 1s shake-up photoelectron spectrum structures. All energies are given relative to the binding energy of the O 1s mainline (539.79 eV). The theoretical energies, intensities, electronic part of second moment and the assignment of the structures is based on the SAC-CI general-*R* calculations performed

Label	Experimental (present)		SAC-CI general-R			
	ΔE	f	ΔE	f	$\langle r^2 \rangle$	Dominant configuration[a]
O 1s	0.000 (539.79)	1.000	0.000 (540.12)	1.000	14	0.90 ($1a_1$)
1	16.96	0.026	16.21	0.006	21	$0.26(3a_1^{-1}8a_1 1a_1^{-1}) - 0.26(1a_1^{-1}8a_1 3a_1^{-1})$
			18.19	0.006	20	$0.44(3a_1^{-1}8a_1 1a_1^{-1}) + 0.44(1a_1^{-1}8a_1 3a_1^{-1})$
2	20.40	0.016	20.66	0.012	33	$0.37(1a_1^{-1}4b_1 1b_1^{-1}) + 0.28(1a_1^{-1}3b_1 1b_1^{-1}) - 0.28(1b_1^{-1}3b_1 1a_1^{-1})$
3	23.07	0.033	23.37	0.004	35	$0.41(1b_1^{-1}4b_1 1a_1^{-1}) + 0.41(1a_1^{-1}4b_1 1b_1^{-1}) + 0.30(1b_1^{-1}3b_1 1a_1^{-1}) + 0.30(1a_1^{-1}3b_1 1b_1^{-1})$
			24.16	0.030	51	$0.34(1b_2^{-1}3b_2 1a_1^{-1}) + 0.30(1b_1^{-1}3b_1 1a_1^{-1})$
4	24.50	0.063	25.28	0.045	79	$0.37(3a_1^{-1}7a_1 1a_1^{-1}) + 0.35(1a_1^{-1}7a_1 3a_1^{-1})$
			25.47	0.002	70	$0.27(1a_1^{-1}8a_1 3a_1^{-1}) + 0.26(3a_1^{-1}4a_1 1a_1^{-1})$
			26.25	0.005	166	$0.25(1a_1^{-1}5a_1 3a_1^{-1}) - 0.25(3a_1^{-1}5a_1 1a_1^{-1})$
5	25.57	0.021	26.50	0.019	213	$0.31(1a_1^{-1}3b_1 1b_1^{-1}) + 0.28(1b_1^{-1}2b_1 1a_1^{-1})$
			27.89	0.010	177	$0.29(1a_1^{-1}2b_1 1b_1^{-1}) - 0.27(1b_1^{-1}2b_1 1a_1^{-1})$
6	28.49	0.021	29.16	0.003	103	$0.48(1a_1^{-1}5a_1 3a_1^{-1}) + 0.47(3a_1^{-1}5a_1 1a_1^{-1})$
			30.42	0.001	100	$0.29(1a_1^{-1}2b_2 1b_2^{-1}) - 0.28(1b_2^{-1}4b_2 1a_1^{-1})$
			33.10	0.006	64	$0.44(1a_1^{-1}5b_1 1b_1^{-1}) - 0.29(1a_1^{-1}12a_1 3a_1^{-1})$
			33.60	0.001	112	$0.43(1a_1^{-1}11a_1 3a_1^{-1}) - 0.34(3a_1^{-1}11a_1 1a_1^{-1})$
			34.11	0.002	216	$0.53(1b_2^{-1}2b_2 1a_1^{-1}) + 0.50(1a_1^{-1}2b_2 1b_2^{-1})$
			35.59	0.005	37	$0.38(1b_1^{-1}5b_1 1a_1^{-1}) + 0.37(1a_1^{-1}6b_2 1b_2^{-1})$
			36.85	0.003	36	$0.30(1a_1^{-1}13a_1 3a_1^{-1}) - 0.30(3a_1^{-1}13a_1 1a_1^{-1})$
			37.76	0.002	48	$0.35(1a_1^{-1}7b_2 1b_2^{-1}) - 0.33(1b_2^{-1}6b_2 1a_1^{-1})$
7	36.19	0.033	38.80	0.012	37	$0.37(1a_1^{-1}6b_2 1b_2^{-1}) + 0.37(1b_2^{-1}6b_2 1a_1^{-1})$
			38.99	0.004	27	$0.30(1a_1^{-1}13a_1 3a_1^{-1}) - 0.30(3a_1^{-1}13a_1 1a_1^{-1})$
			40.41	0.020	31	$0.41(1b_2^{-1}7b_2 1a_1^{-1}) + 0.26(3a_1^{-1}13a_1 1a_1^{-1})$
			41.35	0.066	28	$0.29(2a_1^{-1}8a_1 1a_1^{-1}) + 0.29(1a_1^{-1}8a_1 2a_1^{-1})$
			43.46	0.002	27	$0.17(2a_1^{-1}8a_1 1a_1^{-1}) + 0.17(2a_1^{-1}10a_1 1a_1^{-1})$
			44.10	0.007	37	$0.24(2a_1^{-1}10a_1 1a_1^{-1}) - 0.22(2a_1^{-1}9a_1 1a_1^{-1})$

[a] The configuration $(i^{-1}a\,j^{-1})$ is given by the normalized bonded function $(ia)(j)$ and its spin function is $\frac{1}{\sqrt{2}}(\alpha\beta - \beta\alpha)\alpha$.

4. Results and discussion

In Fig. 1, the experimental O 1s photoelectron satellite spectrum of H_2O (upper panel) is presented and compared with the theoretical spectrum (lower panel) obtained using the SAC-CI general-*R* method. The agreement between the theoretical and experimental spectrum is, in general, very good. For more quantitative comparisons, we have divided the experimental spectrum to components, as shown in the upper panel of Fig. 1, and extracted the values of the energy and integrated intensity for each of the seven components labeled in Fig. 1 as Nos. 1–7. The values obtained from the fitting are compared with the results of the present calculations in Table 1. The last column of Table 1 shows also the dominant configurations of the wavefunction for each of the shake-up states. The configuration is given by the normalized bonded function. The results of the present calculations, showing clearly that the various shake-up states cannot be presented as single configuration states, support the earlier results of Wahlgren [10]: his improved virtual orbital (IVO) calculations including CI predicted a considerable mixing of the configurations.

Referring to the dominant configurations, we can make a conventional assignments for the photoelectron satellite structures Nos. 1–7. The lowest energy peak No. 1 is attributed to the shake-up excitation from the bonding $3a_1$ to the antibonding $8a_1$, while peak No. 2 is due to the shake-up from the non-bonding $1b_1$ to the 3p Rydberg, $3b_1 + 4b_1$. The most prominent structures Nos. 3 and 4 are due to the shake-up to the 3p Rydberg orbitals, that is linear combination of $1b_2$–$3b_2$ and $1b_1$–$3b_1$, and $3a_1$–$7a_1$, respectively. The shoulder structures labeled as Nos. 5 and 6 are assigned to many shake-up states with the transitions to the Rydberg orbitals consisting mainly of O 3p, 4s and 4p orbitals. The broad peak structure No. 7 is assigned as the shake-up from the O 2s like $2a_1$ into the antibonding $8a_1$. These assignments are also consistent with the electronic part of the second moment $\langle r^2 \rangle$. The present assignments based on dominant configurations agree reasonably well with the ones given in the earlier theoretical works [9–12,14].

The most prominent difference between the present and the previous calculations is the intensity distribution of the shake-up transitions. In comparison with the excellent agreement between the present experiment and theory, the theoretical absolute intensities by Wahlgren [10] do not agree well with the experimental results. In other previous works, many close-lying shake-up states seem to be populated, whereas the results of the present calculations suggest that although there are many states in the region of interest, only few of them are highly populated.

It should be noted that since the structures labeled as 5, 6 and 7 are superimposed on the step-like baselines the estimation of the corresponding intensities may be uncertain. Here the baselines are modeled by the arctan functions, which are often used to describe opening of the single ionization channels (see, e.g., Refs. [34,35]). The baselines here represent the shake-off contributions. The baseline that rises at ~25 eV corresponds to the sum of the shake-off from the outer valence orbitals $1b_2$, $3a_1$ and $1b_1$ while the rise of the baseline at ~37.5 eV represents the shake-off contribution from the $2a_1$ orbital.

The present experimental spectrum was measured with much better resolution than the earlier spectra [1,3,11,14,15] recorded using conventional X-ray sources. As a consequence, the present spectrum reveals vibrational structures seen, for example, in the inset of upper panel in Fig. 1. Our trial SAC-CI calculations on vibrational structures, however, revealed that the vibronic coupling makes the theoretical prediction of vibrational structures very difficult. Thus, we discuss the vibrational structures only qualitatively, based on the theoretical adiabatic potential energy surfaces for the shake-up states.

In Figs. 2 and 3, 2D potential energy surfaces of 14 lowest-lying shake-up states are presented along the bond distance $R_{O–H} = 0.9$–1.45 Å with the cut of $\theta_{H–O–H} = 130°$ and 180°, respectively. In the figures, the shake-up states whose shake-up intensities are larger than 0.005 in the Franck–Condon region are shown by the solid lines. Other dotted lines represent the states with smaller shake-up intensities. However, since many avoided cross-

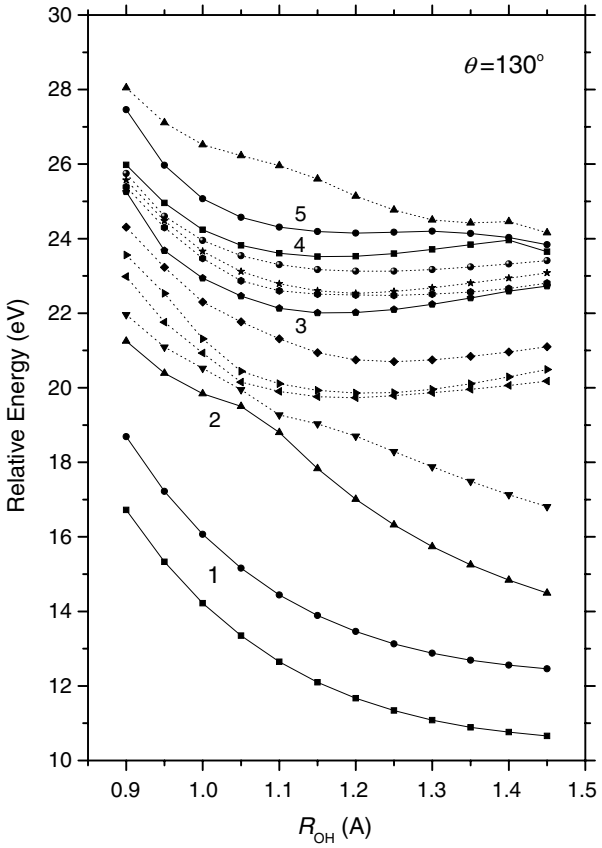

Fig. 2. Potential energy curves of the 14 low-lying A_1 shake-up states accompanying the O 1s ionization of H_2O. The cuts represent the case $R_{O–H} = 0.9$–1.45 Å and $\theta_{H–O–H} = 130°$.

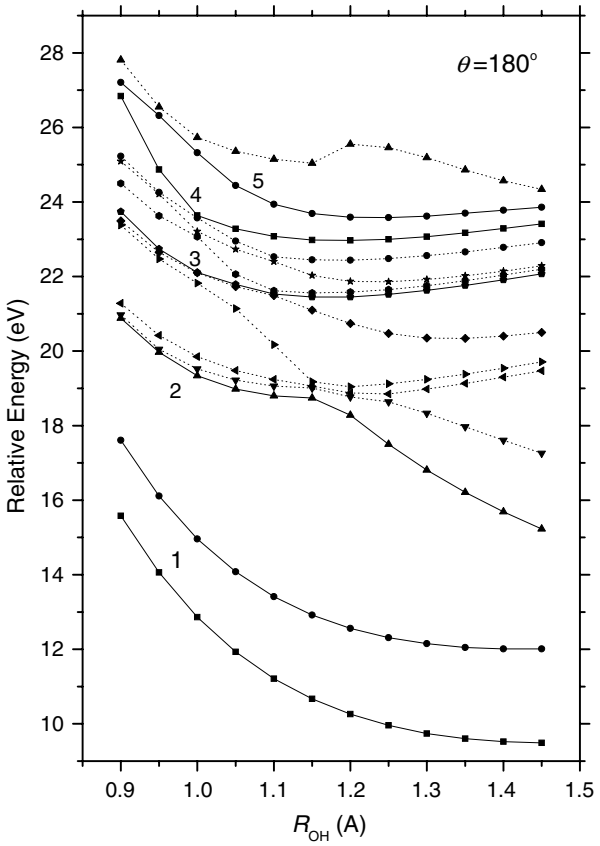

Fig. 3. Potential energy curves of the 14 low-lying A_1 shake-up states accompanying the O1s ionization of H_2O. The cuts represent the case $R_{O-H} = 0.9$–1.45 Å and $\theta_{H-O-H} = 180°$.

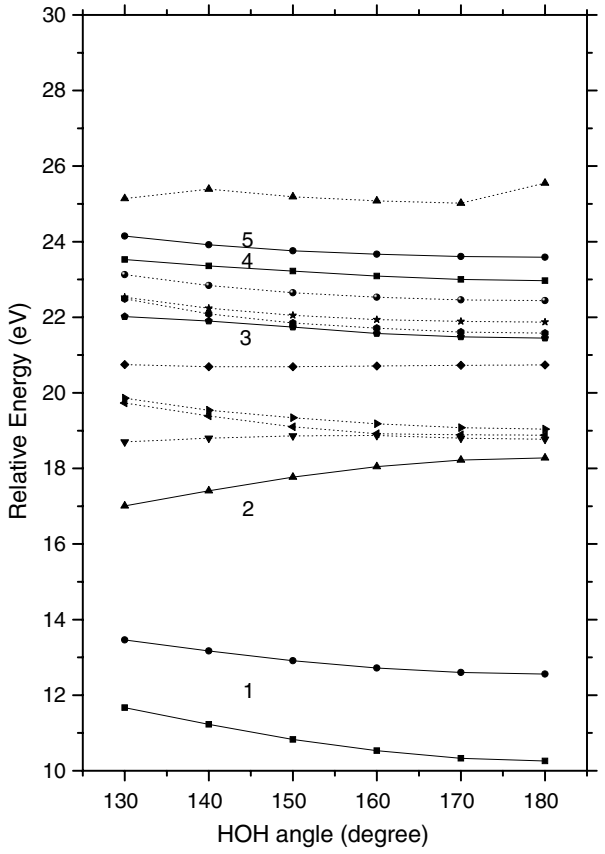

Fig. 4. Potential energy curves of the 14 low-lying A_1 shake-up states; $\theta_{H-O-H} = 130$–$180°$ and $R_{O-H} = 1.2$ Å.

ings occur, some shake-up states with dotted lines also have intensities in particular for the cut $\theta_{H-O-H} = 180°$. These potential energy curves cover the energy region up to about 25 eV relative to main line; namely, up to the shake-up state corresponding to the peak No. 5 in the experimental satellite spectrum. At first glance one may notice a similarity of the two figures. Fig. 4 shows the potential energy curves of the shake-up states along the bond angle $\theta_{H-O-H} = 130$–$180°$ at $R_{O-H} = 1.2$ Å. As represented in this cut, the potential energy surface is very flat for the bending motion, in particular for the states characterized as shake-up to the Rydberg orbital. This flatness explains the similarity of the potential energy curves in Figs. 2 and 3. The linear structure $\theta_{H-O-H} = 180°$ is stable in most of the shake-up states except for the state labeled as No. 2. The bond angle for the O $1s^{-1}$ mainline state in the equilibrium geometry, $\theta_{H-O-H} = 118°$ [23], is larger than that for the neutral ground state, $\theta_{H-O-H} = 104.4°$. The geometry relaxation for the shake-up states becomes larger than that of the mainline state, as seen in Fig. 4, because the atomic dipole force by the lone pair electrons further reduces due to the ionization and excitation.

The following description of the potential surfaces refers to the potential energy curves in Fig. 2 but it is valid also for the 2D potential energy surfaces with angles between 100° and 180° investigated here. The lowest two shake-up states corresponding to satellite peak labeled as No. 1 are dissociative, as expected from the fact that these states are characterized by promotion of the bonding electron to the anti-bonding orbital. The state corresponding to the satellite peak labeled as No. 2 interacts with the higher states and as a result, its potential energy surface becomes repulsive at large internuclear distances, despite the fact that this state is characterized by promotion of the $1b_1$ non-bonding electron to the 3p Rydberg orbital at the small internuclear distance where the transition takes place, i.e., ~0.96 Å. Due to repulsive character of the potential surfaces at large internuclear distances, the corresponding experimental satellite peaks Nos. 1 and 2 are broad without exhibiting any vibrational structures. The potential energy surfaces of the states higher than these states become bound for the symmetric stretching mode. These states are characterized by shake-up to the 3s or 3p Rydberg orbital.

Fig. 5 shows the potential energy curves of the C_s structure along the bond distance $R_{O-H_1} = 1.10$–1.50 Å with $R_{O-H_2} = 1.15$ Å and $\theta_{H_1-O-H2} = 130°$. The curves for the low-lying shake-up states corresponding to the satellite bands Nos. 1 and 2 are repulsive and those for Rydberg transitions are flat or repulsive. The shake-up states corresponding to the Nos. 3 and 4 bands are, however, weakly

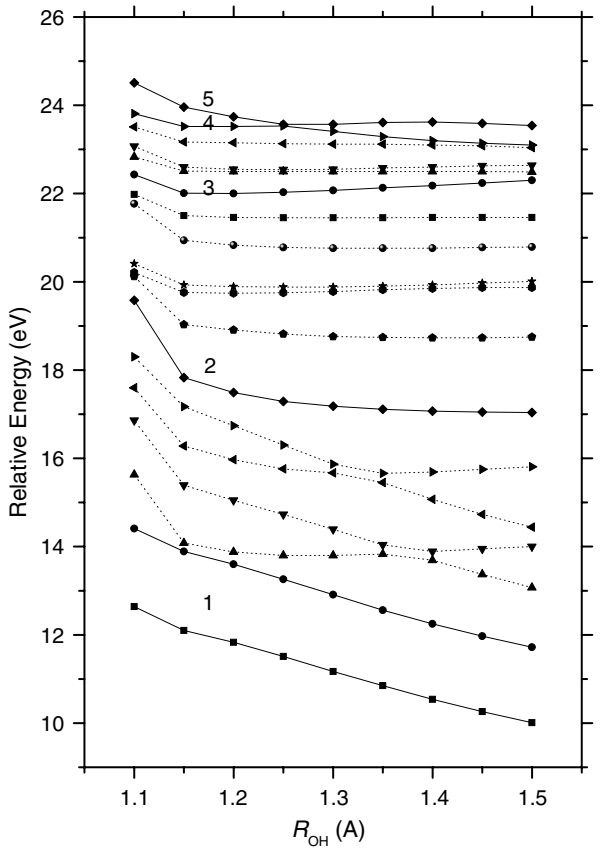

Fig. 5. Potential energy curves of the 18 low-lying A′ shake-up states in C_s structure, $R_{O-H_1} = 1.10$–1.50 Å with $R_{O-H_2} = 1.15$ Å and $\theta_{H_1-O-H2} = 130°$.

bound for this coordinate. Thus, the present ab initio results for the potential energy surfaces of the shake-up states suggest that the vibrational structure can be expected only for the states No. 3 and 4, which are definitely bound along the symmetric stretching coordinate and weakly bound or nearly flat along other coordinates. Indeed the vibrational structure in this extreme situation has been observed experimentally on the low-energy side of the band No. 3. We could not perform the vibrational analysis for this state as pointed out earlier because there are so many shake-up states that can be vibronically coupled within the relevant narrow energy region. However, it is clear that the vibrational structure in the band No. 3 seen in the inset of Fig. 1 can be attributed to that of the bound state with the calculated relative intensity of 0.03 in Table 1.

5. Conclusion

The O 1s photoelectron satellite spectrum of H_2O has been recorded at high resolution and some vibrational structures are detected. The electronic structures of the observed spectrum are assigned reliably with the aid of present ab initio calculations based on the SAC-CI general-*R* method. The present calculations for the potential energy surfaces well elucidate the origin of the vibrational structures observed in the experimental spectrum.

Acknowledgements

The experiment was carried out with the approval of the SPRING-8 program advisory committee. The work was supported in part by Grants-in-Aid for Scientific Research from the Japanese Society for the Promotion of Science (JSPS) and by the Grant for Creative Scientific Research from the Ministry of Education, Science, Culture and Sports of Japan. R.S. and H.A. acknowledge the financial support from the Research Council for Natural Sciences and Engineering of the Academy of Finland. S.L.S. acknowledges the Swedish Research Council (VR) and the Foundation for Strategic Research (SSF).

References

[1] K. Siegbahn, J. Electron Spectrosc. Relat. Phenom. 5 (1974) 3.
[2] U. Gelius, J. Electron Spectrosc. Relat. Phenom. 5 (1974) 985.
[3] K. Siegbahn, C. Nordling, G. Johansson, J. Hedman, P.F. Hedèn, K. Hamrin, U. Gelius, T. Bergmark, L.O. Werme, R. Manne, Y. Baer, ESCA Applied to Free Molecules, North-Holland, Amsterdam, 1969.
[4] L.S. Cederbaum, W. Domcke, J. Schirmer, W. von Niessen, Adv. Chem. Phys. 65 (1986) 115.
[5] J. Tulkki, Phys. Rev. Lett. 62 (1989) 2817.
[6] G. Fronzoni, D. Ge Alti, P. Decleva, J. Phys. B: At. Mol. Opt. Phys. 32 (1999) 5357.
[7] K. Kuramoto, M. Ehara, H. Nakatsuji, M. Kitajima, H. Tanaka, A. De Fanis, Y. Tamenori, K. Ueda, J. Electron Spectrosc. Relat. Pheonom. 142 (2005) 253.
[8] K. Ueda, M. Hoshino, T. Tanaka, M. Kitajima, H. Tanaka, A. De Fanis, Y. Tamenori, M. Ehara, F. Oyagi, K. Kuramoto, H. Nakatsuji, Phys. Rev. Lett. 94 (2005) 243004.
[9] S. Svensson, H. Ågren, U.I. Wahlgren, Chem. Phys. Lett. 38 (1976) 1.
[10] U. Wahlgren, Mol. Phys. 33 (1977) 1109.
[11] D.K. Creber, J.S. Tse, G.M. Bancroft, J. Chem. Phys. 72 (1980) 4291.
[12] R. Arneberg, J. Müller, R. Manne, Chem. Phys. 64 (1982) 249.
[13] H. Ågren, V. Carravetta, J. Chem. Phys. 87 (1987) 370.
[14] N. Mårtensson, P.Å. Malmquist, S. Svensson, E. Basilier, J.J. Pireaux, U. Gelius, K. Siegbahn, Nouv. J. Chim. 1 (1977) 191.
[15] D. Nordfors, A. Nilsson, N. Må rtensson, S. Svensson, U. Gelius, H. Ågren, J. Electron Spectrosc. Relat. Phenom. 56 (1991) 117.
[16] H. Nakatsuji, Chem. Phys. Lett. 59 (1978) 362.
[17] H. Nakatsuji, Chem. Phys. Lett. 67 (1979) 329.
[18] H. Nakatsuji, Computational Chemistry-Review of Current Trends, vol. 2, World Scientific, 1997, pp. 62–124.
[19] H. Nakatsuji, Chem. Phys. Lett. 177 (1991) 331.
[20] M. Ehara, H. Nakatsuji, Chem. Phys. Lett. 282 (1998) 347.
[21] M. Ehara, M. Ishida, K. Toyota, H. Nakatsuji, in: K.D. Sen (Ed.), Reviews in Modern Quantum Chemistry, World Scientific, Singapore, 2002.
[22] K. Kuramoto, M. Ehara, H. Nakatsuji, J. Chem. Phys. 122 (2005) 014304.
[23] R. Sankari, M. Ehara, H. Nakatsuji, Y. Senba, K. Hosokawa, H. Yoshida, A. De Fanis, Y. Tamenori, S. Aksela, K. Ueda, Chem. Phys. Lett. 380 (2003) 647.
[24] T. Tanaka, H. Kitamura, J. Synchrotron Radiat. 3 (1996) 47.
[25] H. Ohashi, E. Ishiguro, Y. Tamenori, H. Kishimoto, M. Tanaka, M. Irie, T. Tanaka, T. Ishikawa, Nucl. Instrum. Meth. A 467 (2001) 529.
[26] H. Ohashi, E. Ishiguro, Y. Tamenori, H. Okumura, A. Hiraya, H. Yoshida, Y. Senba, K. Okada, N. Saito, I.H. Suzuki, K. Ueda, T. Ibuki, S. Nagaoka, I. Koyano, T. Ishikawa, Nucl. Instrum. Meth. A 467 (2001) 533.
[27] K.C. Prince, L. Avaldi, M. Coreno, R. Camilloni, M. de Simone, J. Phys. B 32 (1999) 2551.

[28] S. Sorensen et al. (to be published).
[29] P. Baltzer, L. Karlsson, M. Lundqvist, B. Wannberg, Rev. Sci. Instrum. 64 (1993) 2179.
[30] A. Schaefer, C. Huber, R. Ahlrichs, J. Chem. Phys. 100 (1994) 5829.
[31] T.H. Dunning Jr, P.J. Hay, in: H.F. Schaefer III (Ed.), Methods of Electronic Structure Theory, vol.3, Plenum Press, New York, 1977.
[32] H. Nakatsuji, Chem. Phys. 75 (1983) 425.
[33] M.J. Frisch et al., GAUSSIAN 03, Gaussian Inc., Pittsburgh, PA, 2003.
[34] M. Breinig, M.H. Chen, G.E. Ice, F. Parente, B. Crasemann, G.S. Brown, Phys. Rev. A 22 (1980) 520.
[35] A. De Fanis, N. Saito, H. Yoshida, Y. Senba, Y. Tamenori, H. Ohashi, H. Tanaka, K. Ueda, Phys. Rev. Lett. 89 (2002) 243001.